A non-parametric approach to measuring the $K^-\pi^+$ amplitudes in $D^+ \to K^-K^+\pi^+$ decay

FOCUS Collaboration [1]

J.M. Link [a], P.M. Yager [a], J.C. Anjos [b], I. Bediaga [b], C. Castromonte [b], A.A. Machado [b],
J. Magnin [b], A. Massafferri [b], J.M. de Miranda [b], I.M. Pepe [b], E. Polycarpo [b],
A.C. dos Reis [b], S. Carrillo [c], E. Casimiro [c], E. Cuautle [c], A. Sánchez-Hernández [c],
C. Uribe [c], F. Vázquez [c], L. Agostino [d], L. Cinquini [d], J.P. Cumalat [d], V. Frisullo [d],
B. O'Reilly [d], I. Segoni [d], K. Stenson [d], J.N. Butler [e], H.W.K. Cheung [e], G. Chiodini [e],
I. Gaines [e], P.H. Garbincius [e], L.A. Garren [e], E. Gottschalk [e], P.H. Kasper [e], A.E. Kreymer [e],
R. Kutschke [e], M. Wang [e], L. Benussi [f], S. Bianco [f], F.L. Fabbri [f], A. Zallo [f], M. Reyes [g],
C. Cawlfield [h], D.Y. Kim [h], A. Rahimi [h], J. Wiss [h,*], R. Gardner [i], A. Kryemadhi [i],
Y.S. Chung [j], J.S. Kang [j], B.R. Ko [j], J.W. Kwak [j], K.B. Lee [j], K. Cho [k], H. Park [k],
G. Alimonti [l], S. Barberis [l], M. Boschini [l], A. Cerutti [l], P. D'Angelo [l], M. DiCorato [l], P. Dini [l],
L. Edera [l], S. Erba [l], P. Inzani [l], F. Leveraro [l], S. Malvezzi [l], D. Menasce [l],
M. Mezzadri [l], L. Moroni [l], D. Pedrini [l], C. Pontoglio [l], F. Prelz [l], M. Rovere [l], S. Sala [l],
T.F. Davenport III [m], V. Arena [n], G. Boca [n], G. Bonomi [n], G. Gianini [n], G. Liguori [n],
D. Lopes Pegna [n], M.M. Merlo [n], D. Pantea [n], S.P. Ratti [n], C. Riccardi [n], P. Vitulo [n], C. Göbel [o],
J. Otalora [o], H. Hernandez [p], A.M. Lopez [p], H. Mendez [p], A. Paris [p], J. Quinones [p],
J.E. Ramirez [p], Y. Zhang [p], J.R. Wilson [q], T. Handler [r], R. Mitchell [r], D. Engh [s], M. Hosack [s],
W.E. Johns [s], E. Luiggi [s], M. Nehring [s], P.D. Sheldon [s], E.W. Vaandering [s],
M. Webster [s], M. Sheaff [t]

[a] *University of California, Davis, CA 95616, USA*
[b] *Centro Brasileiro de Pesquisas Físicas, Rio de Janeiro, RJ, Brazil*
[c] *CINVESTAV, 07000 México City, DF, Mexico*
[d] *University of Colorado, Boulder, CO 80309, USA*
[e] *Fermi National Accelerator Laboratory, Batavia, IL 60510, USA*
[f] *Laboratori Nazionali di Frascati dell'INFN, Frascati I-00044, Italy*
[g] *University of Guanajuato, 37150 Leon, Guanajuato, Mexico*
[h] *University of Illinois, Urbana-Champaign, IL 61801, USA*
[i] *Indiana University, Bloomington, IN 47405, USA*
[j] *Korea University, Seoul 136-701, South Korea*
[k] *Kyungpook National University, Taegu 702-701, South Korea*
[l] *INFN and University of Milano, Milano, Italy*
[m] *University of North Carolina, Asheville, NC 28804, USA*
[n] *Dipartimento di Fisica Nucleare e Teorica and INFN, Pavia, Italy*
[o] *Pontifícia Universidade Católica, Rio de Janeiro, RJ, Brazil*
[p] *University of Puerto Rico, Mayaguez, PR 00681, USA*
[q] *University of South Carolina, Columbia, SC 29208, USA*
[r] *University of Tennessee, Knoxville, TN 37996, USA*
[s] *Vanderbilt University, Nashville, TN 37235, USA*
[t] *University of Wisconsin, Madison, WI 53706, USA*

Abstract

Using a large sample of $D^+ \to K^- K^+ \pi^+$ decays collected by the FOCUS photoproduction experiment at Fermilab, we present the first non-parametric analysis of the $K^- \pi^+$ amplitudes in $D^+ \to K^- K^+ \pi^+$ decay. The technique is similar to the technique used for our non-parametric measurements of the $D^+ \to \bar{K}^{*0} e^+ \nu$ form factors. Although these results are in rough agreement with those of E687, we observe a wider S-wave contribution for the $\bar{K}_0^{*0}(1430)$ contribution than the PDG [W.-M. Yao, et al., J. Phys. G 33 (2006) 1], world average mass and width. We have some weaker evidence for the existence of a new, D-wave component at low values of the $K^- \pi^+$ mass.

1. Introduction

This Letter describes a non-parametric measurement of the $K^- \pi^+$ amplitudes present in the decay $D^+ \to K^- K^+ \pi^+$. Charm decay Dalitz plots are traditionally fit using the isobar model where the amplitude is represented by a sum of known Breit–Wigner resonances multiplied by complex amplitudes along with a possible non-resonant term [2]. Often this approach gives a good qualitative representation of the observed populations in the Dalitz plot. The isobar approach, however, does not automatically incorporate some important theoretical constraints. If all final state interactions are dominated by the two-body resonant system, with negligible contribution from the third body, then two-body unitarity is violated by the isobar model. These potential unitarity violations are particularly severe for the case of broad, overlapping resonances.

An alternative, K-matrix formalism spearheaded by the FOCUS Collaboration [7] for charm meson decays, is designed to automatically satisfy unitarity but it is a difficult analysis that requires considerable input from low energy scattering experiments on the form and location of K-matrix poles. In particular, the FOCUS analysis of the D^+, $D_s^+ \to \pi^+ \pi^- \pi^+$ final state used the K-matrix description for just the broad dipion states, but the narrow P-wave states were incorporated as isobar contributions.

This work takes a considerably different approach. We directly measure the $K^- \pi^+$ spin amplitudes as a function of $m_{K^- \pi^+}$ mass by "projecting" them based on the decay angular distribution. Our projective weighting technique, described in Section 3, is very similar to that used to make non-parametric measurements [6] of the q^2 dependence of the helicity amplitudes in $D^+ \to K^- \pi^+ \ell^+ \nu$. In our earlier work, each helicity amplitude is projected by making a weighted histogram of q^2 using special weights designed to block all other amplitude contributions. This projection is done over a set of functions of the $K^- \pi^+$ helicity angle [see Eq. (1)], which is one of the two possible variables to describe a Dalitz plot. The projective weighting technique is therefore an intrinsically one-dimensional analysis. The $D^+ \to K^- K^+ \pi^+$ final state—in principle—is influenced by three amplitudes: $K^- \pi^+$, $K^- K^+$, and even $K^+ \pi^+$. We have chosen the $D^+ \to K^- K^+ \pi^+$ final state as a first test case since the E687 isobar analysis [3] concluded that the observed $D^+ \to K^- K^+ \pi^+$ Dalitz plot could be adequately described by just three resonant contributions: $\phi \pi^+$, $K^+ \bar{K}^{*0}$, and $K^+ \bar{K}_0^{*0}(1430)$. Although $\phi \pi^+$ is an important contribution, the ϕ is a very narrow resonance that can be substantially removed by placing a lower cut on the $m_{K^+ K^-}$ mass (such as $m_{K^+ K^-} > 1050$ MeV/c^2). Because there is no overlap of the ϕ band with the $\bar{K}^{*0}$ band and most of the kinematically allowed $\bar{K}_0^{*0}(1430)$ region, there is a relatively small loss of information from the ϕ-veto. The technique used to correct for residual ϕ contamination is described in Section 5.

Uncertainties in the amplitudes describing the $K^+ K^-$ channel are the major contribution to the systematic error, as discussed in Section 6. The $f_0(980)\pi^+$ amplitude has thus far not been established in $D^+ \to K^- K^+ \pi^+$, but it was found [3] to be a major contributing channel to the related $D_s^+ \to K^+ K^- \pi^+$ decay. A preliminary analysis of the related $D^0 \to K^+ K^- \pi^0$ decay by BaBar [5] indicated a small but significant $f_0(980)\pi^0$ contribution. It is important to establish to what extent other undiscovered contributions in the $K^+ K^-$ channel such as $f_0(980)\pi^+$ could influence these results.[2] Throughout this Letter, unless explicitly stated otherwise, the charge conjugate state is implied when a decay mode of a specific charge is stated.

2. Experimental and analysis details

The data for this Letter were collected in the wideband photoproduction experiment FOCUS during the Fermilab 1996–1997 fixed-target run. In FOCUS, a forward multi-particle spectrometer is used to measure the interactions of high energy photons in

---

* Corresponding author.

E-mail address: jew@uiuc.edu (J. Wiss).

[1] See http://www-focus.fnal.gov/authors.html for additional author information.

[2] Evidence for a small $a_0(980)$ contribution based on an analysis of FOCUS data was reported in a conference proceeding [4].
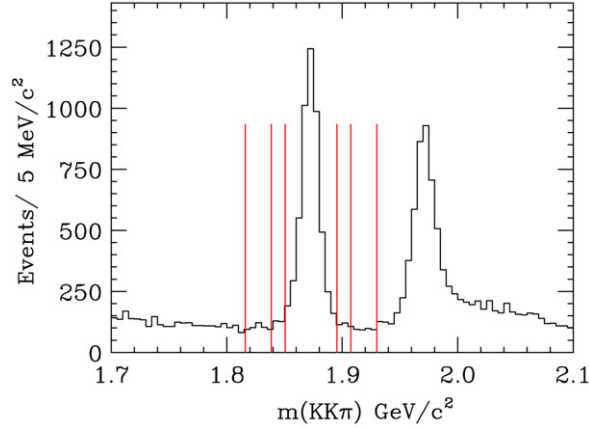
Fig. 1. The $K^-K^+\pi^+$ invariant mass spectra for all of the cuts used in this analysis as well as the ϕ-veto. The $D^+ \to K^-K^+\pi^+$ signal and sideband regions are shown with vertical lines. The peak to the right of the $D^+ \to K^-K^+\pi^+$ peak is due to $D_s^+ \to K^-K^+\pi^+$. The D_s^+ peak appears over a broad, ramped background due to misidentified $D^+ \to K^-\pi^+\pi^+$ decays.

a segmented BeO target. The FOCUS detector is a large aperture, fixed-target spectrometer with excellent track resolution and particle identification. Most of the FOCUS experiment and analysis techniques have been described previously [8–11].

We required that the $K^-K^+\pi^+$ tracks formed a vertex with a confidence level in excess of 10%, and the $K^-K^+\pi^+$ vertex was outside of our BeO target and all other spectrometer material by at least 3σ. Other tracks along with information from the $K^-K^+\pi^+$ "secondary" vertex were used for form a "primary" vertex and the separation between the primary and secondary vertex was required to exceed 7σ. The kaon hypothesis was favored over the pion hypothesis by 3 units of log likelihood in our Čerenkov system for the K^- and K^+ candidates, and the π^+ candidate response was consistent with that for a pion. Finally, we required that the secondary vertex was well isolated. We required that no primary vertex track was consistent with the secondary vertex with a confidence level exceeding 0.5%, and no other track in the event was consistent with the secondary vertex with a confidence level exceeding 1×10^{-4}. In this analysis we eliminated most of the $D^+ \to \phi\pi^+$ contribution by imposing a ϕ-veto that required $m_{K^+K^-} > 1050$ MeV/c^2. Fig. 1 shows the $K^+K^-\pi^+$ invariant mass spectrum after the above selection. We obtained a signal of 6400 $D^+ \to K^-K^+\pi^+$ events prior to the ϕ-veto and 4200 events after the ϕ-veto.

3. Projection weighting technique

The projector method used in this analysis is nearly identical to that used to determine the q^2 dependence of the helicity form factor in $D^+ \to K^-\pi^+\ell^+\nu$ decay [6]. To apply the projector method, we must assume that after we impose the ϕ-veto, the residual effects of the K^-K^+ amplitude contributions are small enough that we can reliably correct for them using the bias technique described in Section 5. In the absence of K^-K^+ resonances, we can write the decay amplitude in terms of $m_{K^-\pi^+} = m$ and the decay angle θ (which is the angle between the K^- and the K^+ in the $K^-\pi^+$ rest frame).

$$A = \sum_{\ell}^{s,p,d,\dots} A_\ell(m) d_{00}^\ell(\cos\theta). \tag{1}$$

Here $d_{00}^\ell(\cos\theta)$ are the Wigner d-matrices that describe the amplitude for a $K^-\pi^+$ system of angular momentum ℓ to simultaneously have 0 angular momentum along its (D^+ frame) helicity axis and the $K^-\pi^+$ decay axis. These angular forms are required to conserve angular momentum for a spinless D^+ to decay into a three pseudo-scalar final state for a given $K^-\pi^+$ angular momentum. For simplicity, we illustrate the technique assuming only P-wave and S-wave contributions although contributions up to and including D-wave are included in the analysis. In the absence of D-wave or higher amplitudes, the decay intensity consists of three terms which depend on the two complex functions: $S(m)$ and $P(m)$ of $m \equiv m_{K^-\pi^+}$.

$$I(m, \cos\theta) = |A|^2 = |S(m) + P(m)\cos\theta|^2 = |S(m)|^2 + 2\,\text{Re}\{S^*(m)P(m)\}\cos\theta + |P(m)|^2\cos^2\theta. \tag{2}$$

For notational simplicity we will write the direct terms as $SS(m) \equiv |S(m)|^2$ and $PP(m) \equiv |P(m)|^2$ and the interference term as $SP(m) \equiv \text{Re}\{S^*(m)P(m)\}$:

$$I(m, \cos\theta) = SS(m) + 2SP(m)\cos\theta + PP(m)\cos^2\theta. \tag{3}$$

Our approach is to divide $\cos\theta$ into twenty evenly spaced angular bins. Let $^i\vec{D} = (^in_1\ {}^in_2\ \cdots\ {}^in_{20})$ be a vector whose 20 components give the population in data for each of the 20 $\cos\theta$ bins. Here ^{i} specifies the ith $m_{K^-\pi^+}$ bin. Our goal is to represent the $^i\vec{D}$ vector as a sum over the expected populations for each of the three partial waves. We will call these $^i\vec{m}$ vectors. For this simplified

case, there are three such vectors computed for each $m_{K^-\pi^+}$ bin: $\{^i\vec{m}_\alpha\} = (^i\vec{m}_{SS}, {}^i\vec{m}_{SP}, {}^i\vec{m}_{PP})$. Each $^i\vec{m}_\alpha$ is generated using a phase space and full detector simulation for $D^+ \to K^- K^+ \pi^+$ decay with one form factor product turned on, and all other form factor products shut off. Hence the $^i\vec{m}_{PP}$ vector is computed assuming an intensity of $\cos^2\theta$ for each $m_{K^-\pi^+}$ bin. The $^i\vec{m}$ vectors incorporate the underlying angular distribution as well as all acceptance and cut efficiency effects. In particular, the ϕ-veto creates substantial inefficiencies at low $\cos\theta$ and high $m_{K^-\pi^+}$, whereas the other cuts have a reasonably uniform acceptance in $\cos\theta$.

We use a weighting technique to fit the bin populations in the data to the form: $^i\vec{D} = F_{SS}(m_i)\,^i\vec{m}_{SS} + F_{SP}(m_i)\,^i\vec{m}_{SP} + F_{PP}(m_i)\,^i\vec{m}_{PP}$. The term $F_{SP}(m_i)$, for example, is proportional to $SP(m_i)$ along with the overall acceptance and phase space for an SP interference term generated in a given m_i bin. Multiplying the $^i\vec{D}$ data vector by each $^i\vec{m}_\alpha$ produces a "component" equation:

$$
\begin{pmatrix} {}^i\vec{m}_{SS}\cdot{}^i\vec{D} \\ {}^i\vec{m}_{SP}\cdot{}^i\vec{D} \\ {}^i\vec{m}_{PP}\cdot{}^i\vec{D} \end{pmatrix} = \begin{pmatrix} \vec{m}_{SS}\cdot\vec{m}_{SS} & \vec{m}_{SS}\cdot\vec{m}_{SP} & \vec{m}_{SS}\cdot\vec{m}_{PP} \\ \vec{m}_{SP}\cdot\vec{m}_{SS} & \vec{m}_{SP}\cdot\vec{m}_{SP} & \vec{m}_{SP}\cdot\vec{m}_{PP} \\ \vec{m}_{PP}\cdot\vec{m}_{SS} & \vec{m}_{PP}\cdot\vec{m}_{SP} & \vec{m}_{PP}\cdot\vec{m}_{PP} \end{pmatrix} \begin{pmatrix} F_{SS}(m_i) \\ F_{SP}(m_i) \\ F_{PP}(m_i) \end{pmatrix}.
$$

The formal solution to this is:

$$
\begin{pmatrix} F_{SS}(m_i) \\ F_{SP}(m_i) \\ F_{PP}(m_i) \end{pmatrix} = \begin{pmatrix} \vec{m}_{SS}\cdot\vec{m}_{SS} & \vec{m}_{SS}\cdot\vec{m}_{SP} & \vec{m}_{SS}\cdot\vec{m}_{PP} \\ \vec{m}_{SP}\cdot\vec{m}_{SS} & \vec{m}_{SP}\cdot\vec{m}_{SP} & \vec{m}_{SP}\cdot\vec{m}_{PP} \\ \vec{m}_{PP}\cdot\vec{m}_{SS} & \vec{m}_{PP}\cdot\vec{m}_{SP} & \vec{m}_{PP}\cdot\vec{m}_{PP} \end{pmatrix}^{-1} \begin{pmatrix} {}^i\vec{m}_{SS}\cdot\vec{D}_i \\ {}^i\vec{m}_{SP}\cdot\vec{D}_i \\ {}^i\vec{m}_{PP}\cdot\vec{D}_i \end{pmatrix}.
$$

This solution can be written as $F_{SS}(m_i) = {}^i\vec{P}_{SS}\cdot\vec{D}_i$, $F_{SP}(m_i) = {}^i\vec{P}_{SP}\cdot\vec{D}_i$, and $F_{PP}(m_i) = {}^i\vec{P}_{PP}\cdot\vec{D}_i$, where the projection vectors are given by:

$$
\begin{pmatrix} \vec{P}_{SS} \\ \vec{P}_{SP} \\ \vec{P}_{PP} \end{pmatrix} = \begin{pmatrix} \vec{m}_{SS}\cdot\vec{m}_{SS} & \vec{m}_{SS}\cdot\vec{m}_{SP} & \vec{m}_{SS}\cdot\vec{m}_{PP} \\ \vec{m}_{SP}\cdot\vec{m}_{SS} & \vec{m}_{SP}\cdot\vec{m}_{SP} & \vec{m}_{SP}\cdot\vec{m}_{PP} \\ \vec{m}_{PP}\cdot\vec{m}_{SS} & \vec{m}_{PP}\cdot\vec{m}_{SP} & \vec{m}_{PP}\cdot\vec{m}_{PP} \end{pmatrix}^{-1} \begin{pmatrix} {}^i\vec{m}_{SS} \\ {}^i\vec{m}_{SP} \\ {}^i\vec{m}_{PP} \end{pmatrix}. \tag{4}
$$

We modify the projector weights to simultaneously correct for cut efficiency, acceptance, as well as the phase space variation required to convert say $F_{SP}(m_i)$ into $SP(m_i)$ as discussed in Ref. [6]. This procedure scales the $^i\vec{P}_{SP}$, for example, into a modified weight $^i\vec{P}'_{SP}$ which includes all acceptance, efficiency corrections, and phase space effects.

The various projector dot products are implemented through a weighting technique. For example, if we are trying to extract the $2\,S(m_{K^-\pi^+}) \times P(m_{K^-\pi^+})$ interference in the ith $m_{K^-\pi^+}$ bin, we need to construct the dot product:

$$
{}^i\vec{P}'_{SP}\cdot{}^i\vec{D} = \left[{}^i\vec{P}'_{SP}\right]_1 {}^i n_1 + \left[{}^i\vec{P}'_{SP}\right]_2 {}^i n_2 + \cdots + \left[{}^i\vec{P}'_{SP}\right]_{20} {}^i n_{20}.
$$

We can do this by making a weighted histogram of $m_{K^-\pi^+}$ where all events that are reconstructed in the first $\cos\theta$ bin are weighted by $^i[\vec{P}'_{SP}]_1$; all events that are reconstructed in the second $\cos\theta$ bin are weighted by $^i[\vec{P}'_{SP}]_2$ etc.

4. Amplitude ambiguity

Table 1 shows the $\cos\theta$ dependences for each of the 3 direct and 3 interference terms for the $S(m_{K^-\pi^+})$, $P(m_{K^-\pi^+})$, and $D(m_{K^-\pi^+})$ amplitudes.

The problem is that these six terms are not independent. The relationship between them is given in Eq. (5).

$$
{}^i\vec{m}_{SD} = \frac{3\,{}^i\vec{m}_{PP} - {}^i\vec{m}_{SS}}{2}. \tag{5}
$$

Hence one cannot make independent projectors of SS, PP, and SD, and must choose two out of these three or the inverse matrix of Eq. (4) will become singular. Since it is known [3] that the $K^-\pi^+$ spectrum in $D^+ \to K^- K^+ \pi^+$ is dominated by the PP contribution ($\bar{K}^{*0}$) and SS contribution [$\bar{K}_0^{*0}(1430)$], we made the choice of dropping the SD interference term and choosing SS, PP, DD, SP, and PD. As a result, the five projectors we use can only partially block any potential SD term. As long as there are no amplitude contributions beyond D-wave, one can show that a potential SD interference contribution will contaminate both the SS and PP spectra but not the two interference terms: SP or PD.

Table 1

The angular distributions for amplitudes up to and including D-wave. Here $\cos\theta$ is the angle between the K^+ and K^- in the $K^-\pi^+$ rest frame. These terms are products of the Wigner d-matrices $d^\ell_{00}(\cos\theta)$

SS	1	PP	$\cos^2\theta$
SP	$\cos\theta$	PD	$\cos\theta(3\cos^2\theta - 1)/2$
SD	$(3\cos^2\theta - 1)/2$	DD	$(3\cos^2\theta - 1)^2/4$

5. The Bias correction

Fig. 2 compares the five reconstructed spectra with the input spectra according to a simulation of the E687 model [3]. The discrepancies between the reconstructed and input spectra are due to residual ϕ contamination in the tail beyond our 1050 MeV/c^2 ϕ-veto. The discrepancies are most prominent at the high end of the $m_{K^-\pi^+}$ distribution (where the ϕ tail is the largest), but are relatively small on the scale of our statistical error elsewhere.

In order to correct for the ϕ tail that extends past $m_{K^+K^-} = 1050$ MeV/c^2, we take the difference between the simulated input and reconstructed spectra as a "bias" that we subtract from the data after normalizing the bias by the ratio of the $\bar{K}^{*0}$ peak area of the PP spectra in the data to that in the simulation.[3] Varying the K^-K^+ amplitudes relative to the E687 model [3] will change the bias correction. Uncertainty in these amplitudes is our major source of systematic error.

6. Systematic errors

The major source of systematic error in this analysis is due to possible uncertainty in the K^-K^+ system amplitudes. In Section 5 we discussed the method used to correct the amplitude spectrum in $K^-\pi^+$ for residual K^-K^+ contributions past our anti-ϕ cut of $m_{K^+K^-} > 1050$ MeV/c^2. This method, however, depends on our model for the K^-K^+ channel. The nominal results assume the ϕ amplitude measured in the E687 [3] analysis as the sole K^-K^+ resonance, but we have considered variations in the result due to differences in the ϕ parameters as well as potential contributions from the $f_0(980)$ and higher mass resonances such as the $f_2(1270)$. The $f_0(980)\pi^+$ amplitude (relative to the $\bar{K}^{*0}$) was varied from 0 to 1 in steps of 0.2 (corresponding to a fit fraction variation from 0 to 20%). The $f_0(980)\pi^+$ relative phase was varied from 0 to 2π in steps of $\pi/4$. The $f_2(1270)\pi^+$ relative amplitude was varied from 0 to 5 in steps of 1 and its phase was varied from 0 to 2π in steps of $\pi/4$. The $\phi\pi^+$ relative phase was varied by 0.9 radian in steps of 0.3 from its nominal value [3] of -2.775. There was no evidence for either a $f_0(980)\pi^+$ or $f_2(1270)\pi^+$ in the E687 analysis of $D^+ \to K^-K^+\pi^+$ decay.

We have considered possible $f_0(980)\pi^+$, $f_2(1270)\pi^+$ contributions and $\phi\pi^+$ parameter variants consistent with our data in four areas: (a) the fraction of $D^+ \to K^-K^+\pi^+$ that appears as $\phi\pi^+$: (b) the shape of the $\cos\theta^*_{K^+\pi^+}$ distribution in the vicinity of the ϕ: (c) agreement with the shape of the complete $m_{K^+K^-}$ spectrum and (d) agreement with the observed populations in
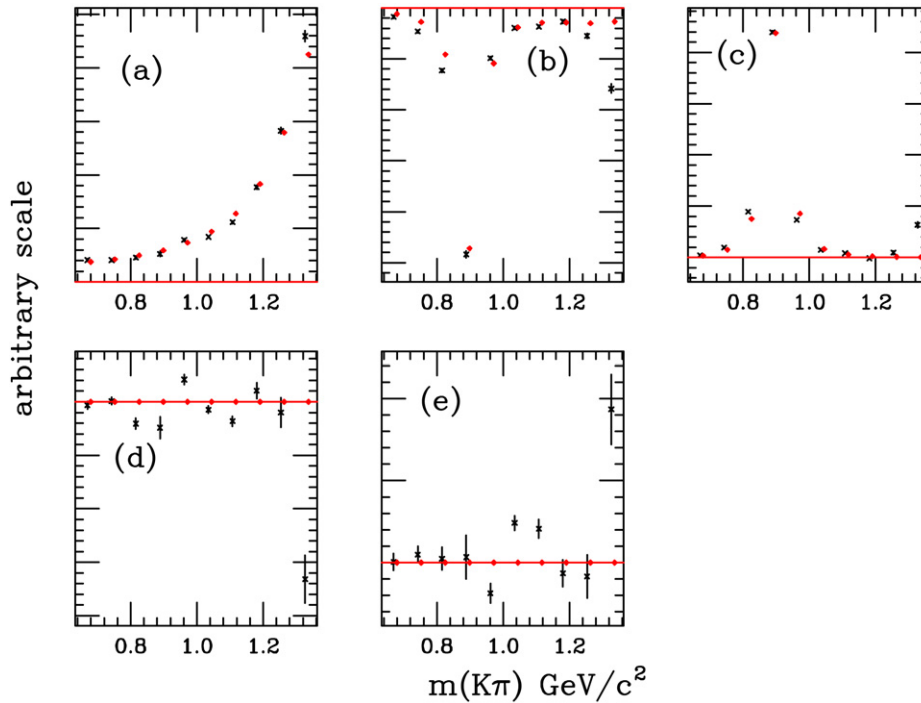

Fig. 2. The first points ("crosses") with error bars show the reconstructed spectra using the method described in Section 3. The closely adjacent points ("diamonds") are the actual $m_{K^-\pi^+}$ spectra used in the simulation based on the model of Ref. [3]. These two Monte Carlo spectra are normalized near the peak bins of the prominent $\bar{K}^{*0}$ present in the PP spectrum. The plots are: (a) $S^2(m_{K^-\pi^+})$ direct term, (b) $2 S(m_{K^-\pi^+}) \times P(m_{K^-\pi^+})$ interference term, (c) $P^2(m_{K^-\pi^+})$ direct term, (d) $2 P(m_{K^-\pi^+}) \times D(m_{K^-\pi^+})$ interference term and (e) $D^2(m_{K^-\pi^+})$ direct term.

---

[3] The normalization is actually done by finding a ratio that minimizes the χ^2 between the data and MC prediction at the peak and one bin on either side of the peak.

two-dimensional bins of the $D^+ \to K^- K^+ \pi^+$ Dalitz plot. Here $\cos\theta^*_{K^+\pi^+}$ is the cosine of the angle between the K^+ and the π^+ tracks in the $K^+ K^-$ rest frame. In each case, the default model with a wide $\bar{K}^{*0}_0(1430)$ and no $f_0(980)$ amplitude was among the best models matching our data according to these tests. Essentially the same set of potential fit variants were selected by the four tests.

We found that a potential $f_0(980)$ when inserted with a phase of $\pi/2$ relative to the $\bar{K}^{*0}(890)$ satisfied our consistency criteria even with a fit fraction as large as 3.3%. Such large $f_0(980)$ amplitudes would be more inconsistent with the data if they came in with a relative phase of zero. We construct the systematic error as the r.m.s. spread of all acceptable fit variants with $f_0(980)$ amplitudes up to 40% of the $\bar{K}^{*0}$ amplitude that both matched the observed binned Dalitz plot populations to within 10σ of the best model and matched the observed $\cos\theta^*_{K^+\pi^+}$ distribution in the vicinity of the ϕ with a confidence level exceeding 1×10^{-4}. Our default model matched the $\cos\theta^*_{K^+\pi^+}$ distribution with a confidence level of 18%. Table 2 in Section 7 compares the sizes of systematic and statistical errors for our five amplitude products. Generally the systematic error was found to be smaller than the statistical error.

A variety of other checks of the results were made during the course of this work. We generated a Monte Carlo using the $m_{K^-\pi^+}$ amplitudes summarized in Table 2 and compared the simulated to the observed $\cos\theta$ distributions as a function of $m_{K^-\pi^+}$ as well as the simulated and observed $m_{K^+K^-}$, $m_{K^-\pi^+}$, and $m_{K^+\pi^+}$ global mass projections. Agreement was good. We also compared the fit results obtained by analyzing the data in different ways. For example, we analyzed the data by constructing only three rather than five projectors and found consistent results with the $S^2(m_{K^-\pi^+})$, $P^2(m_{K^-\pi^+})$, and the $2\,S(m_{K^-\pi^+}) \times P(m_{K^-\pi^+})$ interference terms. We raised the ϕ-veto from $m_{K^+K^-} > 1050\,\text{MeV}/c^2$ to $m_{K^+K^-} > 1100\,\text{MeV}/c^2$ and found consistent results even though the errors in the high mass bins went up dramatically unless the D-wave projectors were excluded.

7. Results

Fig. 3 and Table 2 show the results of this analysis. The relative correlation between the 5 amplitudes is typically less than $\pm 40\%$ except at the highest $m_{K^-\pi^+}$ bins where they are as large as $\pm 65\%$. The comparison plot is based on the E687 analysis [3] but with a much wider $\bar{K}^{*0}_0(1430)$ represented as a Breit–Wigner resonance with a pole at $m_0 = 1412\,\text{MeV}/c^2$ and a width of $\Gamma = 500\,\text{MeV}/c^2$ whereas the world average PDG [1] $\bar{K}^{*0}_0(1430)$ parameters are $m_0 = 1414\,\text{MeV}/c^2$ and $\Gamma = 290\,\text{MeV}/c^2$. In order to roughly reproduce the results in Fig. 3(a), we also increased the magnitude of the $\bar{K}^{*0}_0(1430)$ amplitude by 40% relative to that obtained from the E687 analysis. Hence the curves in Fig. 3 are drawn using a model with a 41.9% $\bar{K}^{*0}_0(1430)$ fit fraction compared to the $37 \pm 3.5\%$ fit fraction quoted in Ref. [3]. The use of a wider $\bar{K}^{*0}_0(1430)$ with a larger amplitude increased the level of the SP interference in the model by 45% to a level in approximate agreement with our data as shown in Fig. 3(b).

8. Summary and discussion

We presented a non-parametric amplitude analysis of the $K^-\pi^+$ system in $D^+ \to K^- K^+ \pi^+$ decay using the technique described in Ref. [6]. There is no need to assume specific Breit–Wigner resonances, forms for mass dependent widths, hadronic form factors, or Zemach momentum factors. As described in Section 3, a set of five weights were generated using Monte Carlo simulations that were designed to project the various amplitude contributions. The five amplitude contributions appear in just five weighted histograms in the $m_{K^-\pi^+}$ mass. Because this is an essentially one-dimensional technique, we chose the $D^+ \to K^- K^+ \pi^+$ final state as a test case. According to an older, traditional Dalitz analysis done in E687 [3] the $D^+ \to K^- K^+ \pi^+$ final state is particularly simple consisting of just $\phi\pi^+$, $\bar{K}^{*0}K^+$, and $\bar{K}^{*0}_0(1430)K^+$. Hence only one narrow resonance, the ϕ, should contribute to the K^-K^+ channel that can be significantly reduced through an ϕ-veto such as $m_{K^+K^-} > 1050\,\text{MeV}/c^2$. This leaves an amplitude that depends primarily on the $K^-\pi^+$ mass. Another attractive feature of the $D^+ \to K^- K^+ \pi^+$ final state is that there should be a

Table 2

Results for the five amplitude contributions. The first error bar is statistical and the second is systematic. All data are arbitrarily scaled by a common factor such that the peak $P^2(m_{K^-\pi^+})$ value near the $\bar{K}^{*0}$ peak is set to 100. Since this is the normalization point it has no systematic error

| $m_{K^-\pi^+}$ (GeV/c^2)	SS	SP	PP	PD	DD
0.633–0.706	$3.79 \pm 1.46 \pm 0.19$	$0.73 \pm 2.03 \pm 0.22$	$-0.06 \pm 3.71 \pm 0.40$	$5.9 \pm 5.25 \pm 0.3$	$3.44 \pm 6.55 \pm 0.68$
0.706–0.779	$1.77 \pm 0.79 \pm 0.33$	$1.83 \pm 1.14 \pm 0.20$	$3.48 \pm 1.99 \pm 0.20$	$-7.8 \pm 2.69 \pm 1.2$	$-4.27 \pm 3.69 \pm 0.36$
0.779–0.852	$1.79 \pm 0.91 \pm 0.26$	$-11.17 \pm 1.38 \pm 0.47$	$19.80 \pm 2.61 \pm 0.70$	$-10.7 \pm 3.4 \pm 0.38$	$-4.27 \pm 4.56 \pm 2.06$
0.852–0.925	$4.79 \pm 1.57 \pm 0.64$	$-38.91 \pm 2.48 \pm 2.06$	$100.00 \pm 4.40 \pm 0.00$	$-5.83 \pm 6.1 \pm 1.62$	$-1.07 \pm 7.68 \pm 2.71$
0.925–0.998	$5.75 \pm 0.90 \pm 0.45$	$-9.73 \pm 1.42 \pm 1.12$	$18.10 \pm 2.40 \pm 1.10$	$0.06 \pm 3.14 \pm 1.7$	$-1.06 \pm 4.06 \pm 2.5$
0.998–1.071	$6.73 \pm 0.77 \pm 0.53$	$-4.27 \pm 1.17 \pm 0.86$	$3.30 \pm 2.10 \pm 1.20$	$-3.92 \pm 2.58 \pm 1.2$	$1.68 \pm 3.39 \pm 0.92$
1.071–1.144	$8.27 \pm 0.90 \pm 0.72$	$-2.07 \pm 1.19 \pm 1.30$	$1.10 \pm 2.20 \pm 1.50$	$-0.45 \pm 3.29 \pm 0.88$	$6.27 \pm 4.02 \pm 0.66$
1.144–1.217	$11.22 \pm 1.29 \pm 1.06$	$-0.79 \pm 1.44 \pm 1.19$	$0.10 \pm 3.30 \pm 1.10$	$-3.09 \pm 5.32 \pm 1.57$	$1.08 \pm 5.87 \pm 0.58$
1.217–1.290	$12.53 \pm 2.13 \pm 1.07$	$-5.31 \pm 2.26 \pm 1.10$	$20.10 \pm 6.70 \pm 2.30$	$-12.77 \pm 9.89 \pm 2.16$	$1.51 \pm 9.47 \pm 1.81$
1.290–1.363	$11.13 \pm 2.87 \pm 2.05$	$3.75 \pm 3.18 \pm 2.11$	$23.70 \pm 8.20 \pm 4.10$	$-4.48 \pm 12.62 \pm 6.31$	$-9.01 \pm 12.68 \pm 2.85$
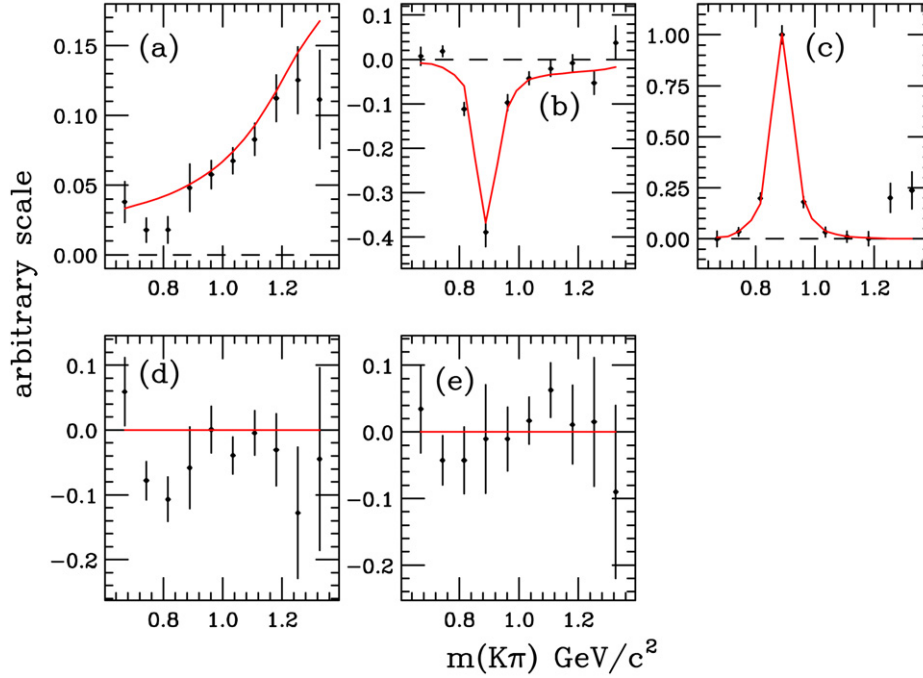
Fig. 3. This figure shows the amplitudes measured in this analysis including systematic errors in 73 MeV/c^2 bins. The default model described in the text are the curves. The data has been normalized such that the $P^2(m_{K^-\pi^+})$ value at the $\bar{K}^{*0}$ mass is 1 in plot (d). The plots are: (a) $S^2(m_{K^-\pi^+})$ direct term, (b) $2\,S(m_{K^-\pi^+}) \times P(m_{K^-\pi^+})$ interference term, (c) $P^2(m_{K^-\pi^+})$ direct term, (d) $2\,P(m_{K^-\pi^+}) \times D(m_{K^-\pi^+})$ interference term and (e) $D^2(m_{K^-\pi^+})$ direct term.

strong S-wave component in the K^-K^+ channel that E687 [3] modeled as the $\bar{K}_0^{*0}(1430)$. Not that much is known about including broad S-wave resonances in charm Dalitz analyzes, and we indeed find considerable discrepancies between our non-parametric description of the S-wave, $K^-\pi^+$ amplitude in $D^+ \to K^-K^+\pi^+$ and the PDG $\bar{K}_0^{*0}(1430)$ mass and width used by E687 [3].

The other possibly significant difference in these results compared to the E687 analysis involves the "glitch" in the first three bins of the $S^2(m_{K^-\pi^+})$ spectrum. We have observed this effect in all variants of the fit we made in the course of understanding systematic errors. The same bins are also present as a glitch in the $2\,P(m_{K^-\pi^+}) \times D(m_{K^-\pi^+})$ interference term which is otherwise consistent with zero. If these are deemed to be significant, one explanation would be the presence of a small D-wave component at low $K^-\pi^+$ masses which could account for both glitches through the mechanism discussed in Section 4 while being small enough to escape notice in the direct $D^2(m_{K^-\pi^+})$ terms where it is second order in the amplitude. Section 4 argues there is an ambiguity in the $\cos\theta$ distributions if one includes waves up to and including D-wave which cannot be eliminated by this or any other method. Hence an $2\,S(m_{K^-\pi^+}) \times D(m_{K^-\pi^+})$ interference term will also affect the $S^2(m_{K^-\pi^+})$ spectrum.

Although the $D^+ \to K^-K^+\pi^+$ decay is an ideal case for an analysis of this kind, it might be possible to extend the analysis to the related $D_s^+ \to K^-K^+\pi^+$ decay[4] as well as $D^0 \to K^+K^-\bar{K}^0$. The emphasis in $D^0 \to K^+K^-\bar{K}^0$ decays would be on studying the $m_{K^+K^-}$ spectrum after applying cuts to minimize the effects of $K^\pm\bar{K}^0$ contributions such as the $a_0^\pm(980)$. One could also use this technique to study the dipion amplitudes present in hadronic four-body decays such as $D^0 \to K^+K^-\pi^+\pi^- \to \phi\pi^+\pi^-$ decay. In particular, one could compare the dipion spectra produced against longitudinally and transversely polarized ϕ's using techniques similar to those described in Ref. [6].

Acknowledgements

---

[4] Care would need to be taken in eliminating or compensating for the $D^+ \to K^-\pi^+\pi^+$ reflection shown in Fig. 1, as well as the $f_0(980)$ and $f_0(1710)$ contributions [3].

References

[1] W.-M. Yao, et al., J. Phys. G 33 (2006) 1.

[2] Dalitz Plot Analysis Formalism by D. Asner, in: W.-M. Yao, et al., J. Phys. G 33 (2006) 1.

[3] R. Greene, Thesis, University of Illinois at Champaign-Urbana, 1995;
P.L. Frabetti, et al., Phys. Lett. B 351 (1995) 591.

[4] S. Malvezzi, D-Meson Dalitz Fit from FOCUS, in: Proceedings of the 7th Conference on Intersection Between Particle and Nuclear Physics CIPANP 2000, Quebec City, 22–28 May 2000, in: AIP Conference Proceedings, vol. 549, 2002, pp. 569–574.

[5] K. Mishra, Studies of Charm Meson Decays at BaBar, DPF, 2006.

[6] FOCUS Collaboration, J.M. Link, et al., Phys. Lett. B 633 (2006) 183;
CLEO Collaboration, Phys. Rev. D 74 (2006) 052001.

[7] FOCUS Collaboration, J.M. Link, et al., Phys. Lett. B 585 (2004) 200.

[8] E687 Collaboration, P.L. Frabetti, et al., Nucl. Instrum. Methods A 320 (1992) 519.

[9] FOCUS Collaboration, J.M. Link, et al., Nucl. Instrum. Methods A 484 (2002) 270.

[10] FOCUS Collaboration, J.M. Link, et al., Nucl. Instrum. Methods A 484 (2002) 174.

[11] FOCUS Collaboration, J.M. Link, et al., Nucl. Instrum. Methods A 516 (2004) 364.